Studies on Spherulitic Morphology and Crystallization Kinetics of Poly(3-hydroxybutyrate) Blended with a Medium-Molecular-Weight Poly(ethylene oxide)

Trong-Ming Don[1]*, Pi-Che Chen[1], Wei-Wei Shang[1] and Hsiu-Jung Chiu[2]

[1]*Department of Chemical and Materials Engineering, Tamkang University,*
Tamsui, Taiwan 251, R.O.C.
[2]*Department of Chemical and Materials Engineering, Ta Hwa Institute of Technology,*
Chiunglin, Hsinchu 30703, Taiwan, R.O.C.

Abstract

Spherulitic morphology and crystallization kinetics of poly(ethylene oxide)/poly(3-hydroxybutyrate) blends, PEO/P(3HB), were investigated using differential scanning calorimeter (DSC), polarized optical microscope (POM) and scanning electronic microscope (SEM). A single glass transition temperature was observed for all the blends and the Gordon-Taylor equation follows the T_g-composition dependence very well. Furthermore, the melting point of P(3HB) was depressed by the addition of PEO component and from which the interaction parameter χ_{12} was calculated to be -0.059 using the Nishi-Wang equation. Thus, it can be concluded that P(3HB) and PEO are miscible in the level of molecular mixing. From POM and SEM observations, P(3HB) spherulites exhibit a banded texture due to the twisting of lamellar crystals. The band spacing is almost a constant, ca. 20 μm, when the crystallization temperature is below 90 °C, at which the maximum growth rate of P(3HB) spherulites occurs. When P(3HB) is blended with PEO, the growth rate of P(3HB) spherulites decreases because of the dilution effect and a decrease in the degree of undercooling. According to the polymer-diluent theory, the nucleation factor K_g and the folded surface free energy σ_e of P(3HB) crystals are calculated to be 5.648×10^5 K^2 and 47.2 erg/cm^2, respectively. Both values decrease when PEO is added.

Key Words: Poly(3-hydroxybutyrate), Poly(ethylene oxide), Blends, Spherulite

1. Introduction

Microbial polyesters, poly(hydroxyalkanoates) (PHAs), have received considerable attention, especially for potential application as biodegradable polymers. Bacteria usually accumulate PHAs in response to nutritional limitations and in the presence of an excess of carbon [1−3]. A variety of Gram-positive and Gram-negative bacteria can produce PHAs as an intracellular storage material of carbon source and energy. They are deposited in the cell cytoplasm as water-insoluble granules that are typically 0.2-0.8 μm in diameter [2−5]. At present, at least 100 different monomeric units as constituents of PHAs have been identified where the composition of PHA depends on the bacterial strain, carbon source and fermentation conditions. Among them, poly(3-hydroxybutyrate) homopolymer, P(3HB), is the most common microbial polyester produced by various microorganisms in nature. The microbial P(3HB) has a completely isotactic structure with only the R-configuration. This means that solutions or films of P(3HB) will rotate the plane of polarized light passing through them. P(3HB) typically forms spherulites when crystallized from the melt in bulk and it generally has a crystallinity ranging from 50 to 80%. The

---

*Corresponding author. E-mail:tmdon@mail.tku.edu.tw tensile strength and Young's modulus of P(3HB) are 43 MPa and 3.5 GPa, respectively, which are close to the mechanical properties of isotactic poly(propylene). However, the elongation at break for P(3HB) is only about 5%, appreciably lower than that of poly(propylene) (~400%). Therefore, PHB is regarded as a plastic with brittleness. Another shortcoming of P(3HB) as regards plastics and fiber applications is its thermally unstable at temperatures immediately above its melting point (T_m) due to the β-elimination reaction. Thus blending of P(3HB) with suitable polymers may offer the opportunity to obtain cheaper products along with improved mechanical properties.

Polymer blends are physical mixtures of different polymers, which they can form either a homogeneous or heterogeneous phase in the amorphous region on a microscopic scale at equilibrium. The former is considered to be miscible, and the latter immiscible. According to the thermodynamic and kinetic behavior of mixing and crystallization process, blends can be arranged to a variety of morphologies, which in turn is a very important factor that affects the mechanical behavior of blends. In the crystalline/amorphous blends, the morphology is resulted by liquid-solid phase separation. The morphological patterns can be characterized by the distance of the segregation of the amorphous diluent. Three basic types are defined: (1) interlamellar segregation, where segregation of the amorphous diluent occurs at the lamellar level; (2) inter-fibrillar segregation, where the amorphous diluent is segregated by a larger distance to the regions between the lamellar bundles in spherulites; (3) interspherulitic segregation, where the amorphous diluent is segregated by the largest distance to the regions between spherulites [6–8]. Thus the amorphous diluent may be trapped in interfibrillar or interlamellar regions within the spherulites or rejected during the crystallization in interspherulitic domains. The position and the extent of dispersion of the amorphous component can be predicted qualitatively through the Keith and Padden parameter $\delta = D/G$, where δ is the segregation parameter, D and G are the diffusion coefficient of the amorphous component and the linear growth rate of spherulites, respectively [9]. Depending on the relative values of D and G, the amorphous diluent may reside between lamellae, fibrils or within the spherulites.

Crystallization kinetics in melt-miscible blends of crystalline/amorphous polymers with P(3HB), such as P(3HB)/poly(epichlorohydrin) [10,11], P(3HB)/poly(vinyl acetate) [12–14], and P(3HB)/atactic-P(3HB) [15, 16], P(3HB)/poly(vinyl phenol) [17,18], has been extensively studied. The thermal and microscopic analysis of these systems has shown a depression of crystallization kinetics of P(3HB) with the addition of amorphous diluent. Though the melt-miscible crystalline/crystalline blends with P(3HB), such as P(3HB)/poly(ethylene oxide) (PEO) [19–22], have also been studied, many experimental and theoretical questions are still needed to be resolved. The morphology of crystalline/crystalline blends is expected to be more complex than that of crystalline/amorphous systems due to the interplay between two crystallization processes. In the previous paper, we have studied the spherulitic morphology and crystallization kinetics of the blends of P(3HB) with a low-molecular-weight PEO (Mw = 5,000) by differential scanning calorimeter and polarized optical microscopy [22]. The isothermal crystallization temperatures studied were in the range between 40 °C and 85 °C. When the blends underwent crystallization at $T_c = 70$ °C, above the melting point of PEO, banded spherulitic texture of P(3HB) was observed, which could be perturbed by the subsequent PEO crystallization in the blends with PEO-rich compositions upon further cooling to room temperature. When the blends were allowed to be crystallized at temperatures below the melting point of PEO, fairly competitive crystallization was observed where crystallization and segregation of PHB and PEO may simultaneously occur, leading to complicated spherulitic morphology. As for the results of crystallization kinetics, the P(3HB) crystallization kinetics exhibited maxima in their dependences of PEO composition. This was attributed to the coupling between enhanced chain mobility and depression in equilibrium melting point. In this article, the spherulitic morphology and crystallization kinetics of P(3HB) with a medium-molecular-weight PEO (M_v = 100,000) were studied in a broader range of temperature, from 40 to 110 °C, since our results show that the maximum growth rate of P(3HB) was near 90 °C.

2. Experimental

2.1 Materials and Sample Preparation

P(3HB) and PEO were supplied by Aldrich Chemical Co. The molecular weight of P(3HB) was measured by gel permeation chromatography, where P(3HB) was first dissolved in chloroform at 80 °C for 40 min and then it was injected to the GPC column. The measured M_n and M_w of P(3HB) based on polystyrene standard were 250,100 and 369,400, respectively. The viscosity average molecular weight (M_v) of PEO was 100,000. P(3HB) was blended with PEO by a solution casting method. The blending components were dissolved in chloroform (0.2 g/15mL) at 80 °C for 40 min in a rotary oven. The solution was subsequently poured onto a Petri dish and the blend film was obtained after evaporating most of the solvent on a hot plate at ca. 90 °C. The blend film was further dried in a vacuum oven at 40 °C for at least 24 h until a constant sample weight.

2.2 Polarized Optical Microscopy

The morphology of spherulites and their growth rate were monitored with an Olympus CX41 polarized optical microscope. The sample film (ca. 109 ± 12 μm thick) was first melt on a Linkam THMS 600 hot stage at 200 °C for 2 min, then quickly quenched to the desired crystallization temperature (T_c) by the purging of liquid nitrogen, where spherulitic growth was monitored. Micrographs were taken at various time periods for measuring the radius of spherulites (R). The growth rate was calculated from the change of radius with time (dR/dt).

2.3 Scanning Electron Microscopy

Low voltage (3-5 kV) scanning electron microscope (FESEM, Leo 1530, Germany) was used to observe the surface morphology of the blends. The sample film was first melt on a Linkam THMS 600 hot stage at 200 °C for 2 min, and then quickly removed to a precision oven set at the desired crystallization temperature. After 3 days for a complete crystallization, the sample film was taken out for SEM observation. Some samples were etched with cold water at 5 °C for 2 days to remove PEO component as much as possible. All specimens were coated with a conductive layer of sputtered gold.

2.4 Differential Scanning Calorimetry (DSC)

To determine the thermal transition temperatures, DSC 2920 from TA Instrument was employed. For measuring transition temperatures, sample was first melted on a hot stage (Linkam THMS 600) at 200 °C for 2 min, and then rapidly quenched with liquid N_2 to avoid the crystallization in the sample as much as possible. Subsequently, the sample was rapidly transferred into DSC cell and heated to 200 °C at a heating rate of 10 °C/min under a nitrogen atmosphere with a flow rate of 50 mL/min. A mid-point method was employed to determine the glass transition temperature (T_g). To determine the equilibrium melting point (T_m°), each sample was first melted on a hot stage at 200 °C for 2 min, and then rapidly transferred into DSC cell equilibrated at the desired crystallization temperature (T_c). After a sufficient time for complete crystallization, the sample was then heated to 200 °C at a heating rate of 10 °C/min. Melting point (T_m) was taken as the endothermic peak value in the thermogram.

3. Results and Discussion

3.1 Miscibility of PEO and P(3HB)

The glass transition temperatures of PEO and P(3HB) are -54.4 °C and -2.5 °C, respectively, as measured by differential scanning calorimeter. Blends of PEO and P(3HB) were obtained by solution casting from chloroform. The blends exhibit a single glass transition temperature in the whole composition range as shown in Figure 1, indicating a complete miscibility of the two components in the amorphous phase. The dependence of T_g on the compositions is well described by the Fox equation (Eq. 1) or Gordon-Taylor equation (Eq. 2):

$$\frac{1}{T_{g,Blend}} = \frac{w_1}{T_{g,1}} + \frac{w_2}{T_{g,2}} \tag{1}$$

$$T_{g,Blend} = \frac{w_1 T_{g,1} + k w_2 T_{g,2}}{w_1 + k w_2} \tag{2}$$

where $T_{g,blend}$, $T_{g,1}$ and $T_{g,2}$ are T_gs of the blend, PEO, and P(3HB), respectively, while w_1 and w_2 are the weight fractions of PEO and P(3HB). Considering the difference between P(3HB) and PEO in heat-capacity change at T_g ($k = \Delta C_{p,PHB}/\Delta C_{p,PEO}$), Gordon-Taylor equation fits exactly along the experimental data, and is better than Fox equation. This T_g-composition dependence was consistent with the results reported in a previous paper [22]. Furthermore, since Fox equation or Gordon-Taylor equation can well describe the T_g-composition dependence, it is suggested that there is no or only weak interaction between PEO and P(3HB).

The miscibility of these two components is also confirmed by the observation of the depression of the equi-

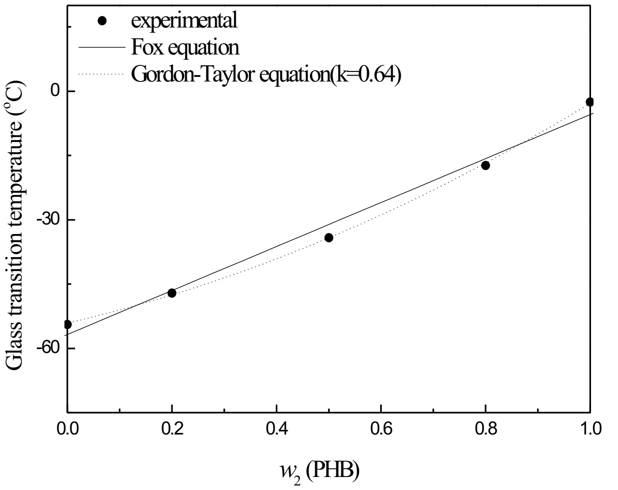

Figure 1. T_g-composition dependence of PEO/P(3HB) blends. ω_2 is weight fraction of P(3HB) component.

librium melting point of P(3HB) component. To determine the equilibrium melting temperature of each blend, Hoffmann-Weeks equation was used:

$$T_m = T_m^\circ(1-\frac{1}{\gamma})+\frac{T_c}{\gamma} \qquad (3)$$

where γ is a constant, T_m is the apparent melting temperature after crystallization at a certain temperature (T_c) and T_m° is the equilibrium melting temperature of a perfect crystal having infinite thickness. By plotting the experimental melting point T_m against the isothermal crystallization temperature T_c at which crystallization took place, T_m° can be obtained as the intersection point of the experimental line with the line $T_m = T_c$. The plot of pure P(3HB) is shown in Figure 2. The equilibrium melting temperature of neat PHB is 187 °C. Though this value is slightly lower than the literature value, it is still in a reasonable range [10]. In the presence of PEO, the equilibrium melting temperature of P(3HB) was strongly depressed, as listed in Table 1. The depression of melting point allows processing the blends at lower temperatures with respect to the neat P(3HB), avoiding the degradation of PHB. The relationship describing the depression of melting point and the interaction parameter χ_{12} between the two polymer components has been established as the Nishi-Wang equation [23]:

$$\frac{1}{T^\circ_{m,b}}-\frac{1}{T^\circ_{m,PHB}} = -\frac{R}{\Delta H_f^o}\frac{V_2}{V_1}\left[\frac{\ln\phi_2}{n_2}+(\frac{1}{n_2}-\frac{1}{n_1})\phi_1+\chi_{12}\phi_1^2\right] \qquad (4)$$

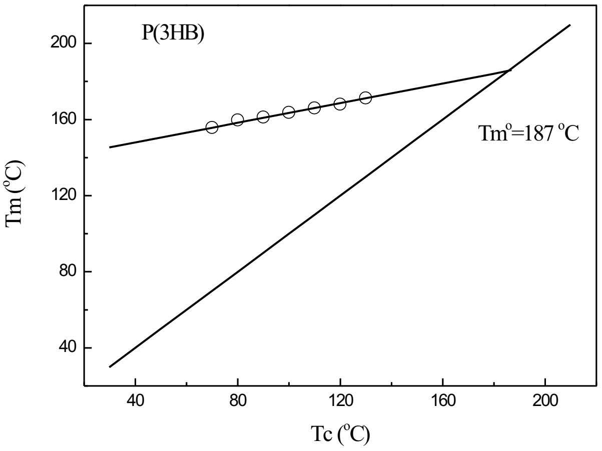

Figure 2. Plot of apparent melting point (T_m) with crystallization temperature (T_c) to determine the equilibrium melting point (T_m°) of P(3HB).

Table 1. Volume fraction of PEO component (ϕ_1), equilibrium melting temperature of P(3HB) component (T_m°) and interaction parameter value (χ_{12}) of PEO/P(3HB) blends

w_1	ϕ_1	T_m° (°C)	χ_{12}
0	0	187	----
0.2	0.213	174	-1.258
0.5	0.520	169	-0.295
0.8	0.813	167	-0.134

Densities of amorphous PEO and P(3HB) are 1.08 and 1.17 g/cm^3, respectively.

where $T_{m,b}^\circ$ and $T_{m,PHB}^\circ$ are the equilibrium melting points of the P(3HB) component in the blend and in the pure state, respectively, ΔH_f° is the theoretical heat of fusion of P(3HB) with 100% crystallinity, V_1, n_1, ϕ_1 and V_2, n_2, ϕ_2 are the molar volume of the repeating unit, the degree of polymerization and the volume fraction of the PEO and P(3HB), respectively. This equation can be applied to PEO/P(3HB) blends as long as the T_c investigated here is above the T_m of PEO (65.7 °C), at which PEO is present as an amorphous component under such conditions. To obtain χ_{12}, the equation was rewritten as follows:

$$\alpha = \frac{\Delta H_f^o}{R}\frac{V_1}{V_2}(\frac{1}{T^\circ_{m,b}}-\frac{1}{T^\circ_{m,PHB}})+\frac{\ln\phi_2}{n_2}+(\frac{1}{n_2}-\frac{1}{n_1})\phi_1 = -\chi_{12}\phi_1^2 \qquad (5)$$

From the plot of left-hand side of the above Equation versus ϕ_1^2, a straight line is obtained with a positive slope as shown in Figure 3, using the values of $T_{m,b}°$ and $T_{m,PHB}°$ derived from the Hoffmann-Weeks method (Table 1), and $n_1 = 2273$, $n_2 = 4295$, and the literatures values of $\Delta H_f° = 1.25 \times 10^4$ J/mol, $V_1 = 40.7$ cm^3/mol, $V_2 = 73.4$ cm^3/mol [19]. The interaction parameter χ_{12} is the opposite of the slope, equal to -0.059, in agreement with the literature values [19]. The negative value of the interaction parameter suggests the miscibility of PEO and P(3HB) components, though the value is so close to zero. However, the intercept is not equal to zero, suggesting that χ_{12} is dependent on the composition. The χ_{12} values at different compositions are also calculated separately and listed in Table 1. They are all negative and slightly increased with increasing concentration of PEO component. From the studies of T_g-composition dependence and the melting point depression, it can be concluded that P(3HB) and PEO are miscible in the level of molecular mixing, though the enthalpic interaction between these two components is weak.

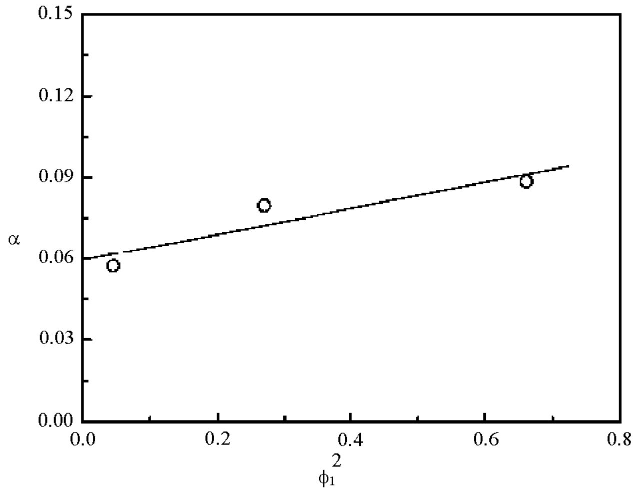

Figure 3. Plot of left-hand side of equation (5),

$$\alpha = \frac{\Delta H_f^{\circ}}{R}\frac{V_1}{V_2}\left(\frac{1}{T_{m,b}^{\circ}} - \frac{1}{T_{m,PHB}^{\circ}}\right) + \frac{\ln \phi_2}{n_2} + \left(\frac{1}{n_2} - \frac{1}{n_1}\right)\phi_1,$$

versus ϕ_1^2 to determine the interaction parameter χ_{12}. ϕ_1 is volume fraction of PEO.

3.2 Spherulitic Morphology

The morphology and growth rate of spherulites were evaluated with a polarized optical microscope (POM). Clearly observed were different behaviors for PEO and P(3HB) undergoing crystallization. For PEO, all the spherulites were nucleated at the same time and the boundaries between them were straight, indicating a heterogeneous nucleation mechanism. However, P(3HB) spherulites were nucleated at different times so that they were different in size when impinging on one another and their boundaries were hyperbolas. In addition, compared to other thermoplastics, the nucleation density is relatively low mostly because of its natural origin. This leads to greater diameter of the spherulites which intends to brittle the material. A Maltese-cross pattern is clearly observed for all PEO and P(3HB) samples, where the arms of cross parallel to the directions of polarizer and analyzer. Figure 4 shows the observed spherulites of neat P(3HB) at several crystallization temperatures. Under the same field, the number of spherulites increases with decreasing the crystallization temperature, due to the increase in the nucleation density. Consequently, smaller spherulites are observed at lower crystallization temperatures. For example, the diameter of P(3HB) spherulites decreases from 1.2 mm at 90 °C to 50 μm at 40 °C. Due to the twisting of lamellar crystals, where the crystallographic a axis is radial, while b and c axes rotating about it [24], P(3HB) spherulites exhibit a banded texture, which shows alternative bright and dark rings under POM. For the present system, the band spacing is almost a constant, ca. 20 μm, when the crystallization temperature is below 90 °C. At temperatures higher than 90 °C, the band spacing of lamellar twisting increases with increasing temperature; eventually, the ring pattern seems to diffuse. For example, the band spacing is ca. 30 μm at 95 °C and 49 μm at 100 °C. Schultz and Kinloch proposed that lamellar twisting may be caused by queues of giant screw dislocation of the same band [25]. However, a recent study by Xu et al. on poly(3-hydroxybutyrate-*co*-3-hydroxyhexanoate) copolymer [26] shows that the lamellae twist before screw dislocation appear, demonstrating that screw dislocation are not causal of twisting. The ultimate driving force for lamellae twisting is still an open question.

Another significant feature in P(3HB) spherulites is the appearance of apparent cracks in some samples when crystallized at high temperatures. Especially, circumferentially cracks are clearly observed at samples during spherulitic growth at temperatures above 90 °C. These apparent cracks appeared as black lines in the optical microscope. It was suggested by Hobbes et al. [27] that the apparent cracks formed in spherulites are due to differences

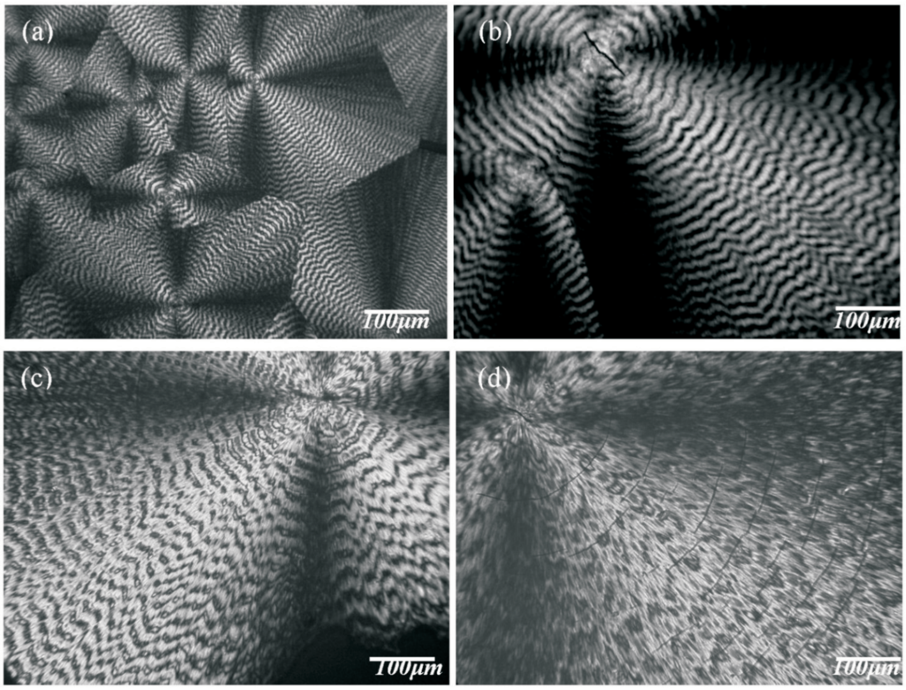

Figure 4. Optical micrographs of banded spherulitic structures of P(3HB) crystallized at (a) 65 °C, (b) 85 °C (c) 95 °C (d) 100 °C.

in thermal expansion between the P(3HB) film and the constraining glass slides. In addition to the circumferentially cracks, a crack at the center of spherulites is also observed.

P(3HB) and PEO are both crystalline polymers with melting points of 175.6 and 65.7 °C, respectively, measured by DSC at a heating rate of 10 °C/min. At temperatures between 65.7 and 175.6 °C, the blend is a crystalline/amorphous system but it becomes as a crystalline/crystalline system below 65.7 °C. Figure 5 shows the banded P(3HB) spherulites of neat P(3HB) and PEO/

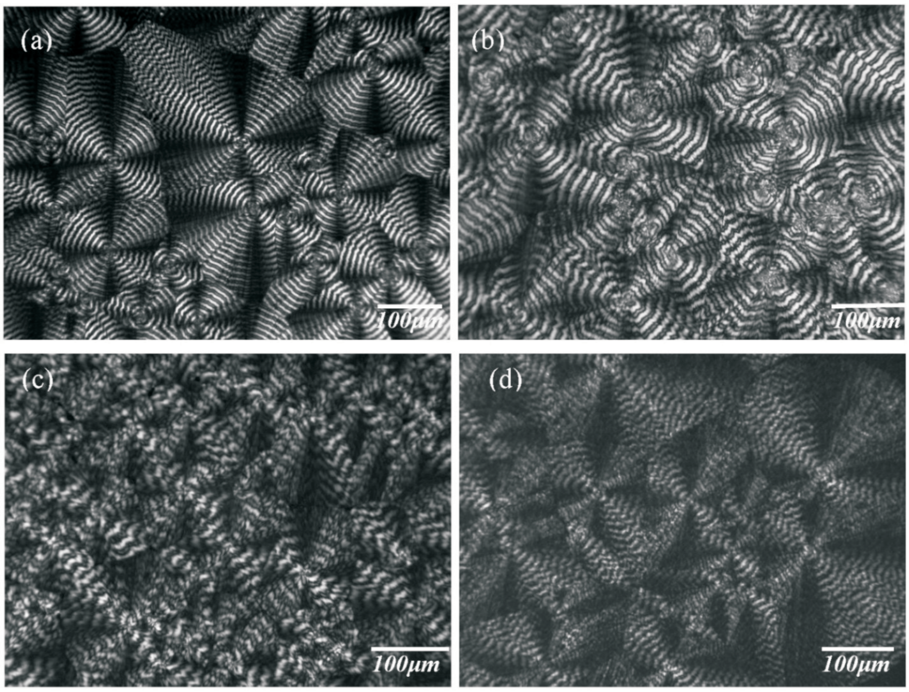

Figure 5. Optical micrographs of banded spherulitic structures of P(3HB) in PEO/P(3HB) blends crystallized at 70 °C, PEO/P(3HB) = (a) 0/100 (b) 20/80 (c) 50/50 (d) 80/20.

P(3HB) blends crystallized at 70 °C. For all the compositions studied, volume-filling spherulites are observed when the samples were allowed to crystallize for a sufficient period of time. Furthermore, the spherulite radius of P(3HB) increased linearly with time and no apparent evidence of liquid-liquid phase separation was found up to the point of spherulite impingement. This implies that PEO was contained within the P(3HB) spherulites during P(3HB) crystallization at 70 °C. Figure 5 also shows that the band spacing in P(3HB) spherulites increased with PEO content and became diffuse. This has the same trend as increasing the crystallization temperature above 90 °C. When the blends were allowed to crystallize at temperatures below the melting point of PEO component, both PEO and P(3HB) crystallized at the same time. Figure 6 shows the spherulitic morphology of PEO/P(3HB) blends crystallized at 50 °C. In contrast to that in the crystalline/amorphous blends, a course spherulitic texture with a disruption of Maltese-cross pattern for all the blends studied was observed. The disruption of Maltese-cross pattern indicates an intra-spherulitic segregation may occur during the crystallization of PEO and P(3HB). Further crystallization of PEO thus could occur in the P(3HB) interfibrillar regions, as well as P(3HB) in the PEO interfibrillar regions.

SEM pictures were taken to facilitate the observation of spherulitic structures. Figure 7 shows the SEM pictures of the PEO/P(3HB) blend (5/5) crystallized at 40 °C for 3 days and etched with cold water for 2 days. A ring structure, characterization of banded texture of P(3HB) spherulites, with a spacing of 10-20 μm was observed. This is in the same magnitude order with that in POM pictures. After etching with cold water that would only remove PEO component, radial cracks were observed in P(3HB) crystallites. This again suggests that PEO component resides in the interfibrillar regions. Chiu and You [28] studied the lamellar morphology of PEO/P(3HB) blends via small angle X-ray scattering (SAXS) and found that amorphous PEO was located in the interfibrillar regions of P(3HB) and the extent of interfibrillar segregation increased with increasing PEO composition.

3.3 Growth Rate of Spherulites

The development of spherulites was monitored, in which radius of spherulites was measured at various times. Figure 8 shows the relationship of spherulitic growth rate (G) with crystallization temperature (T_c) for neat P(3HB) and PEO/P(3HB) blends. The maximum growth rate was found at 90 °C ($T_{c,max}$) for neat P(3HB), which agrees to the previous reports [15,16,29]. It is known that

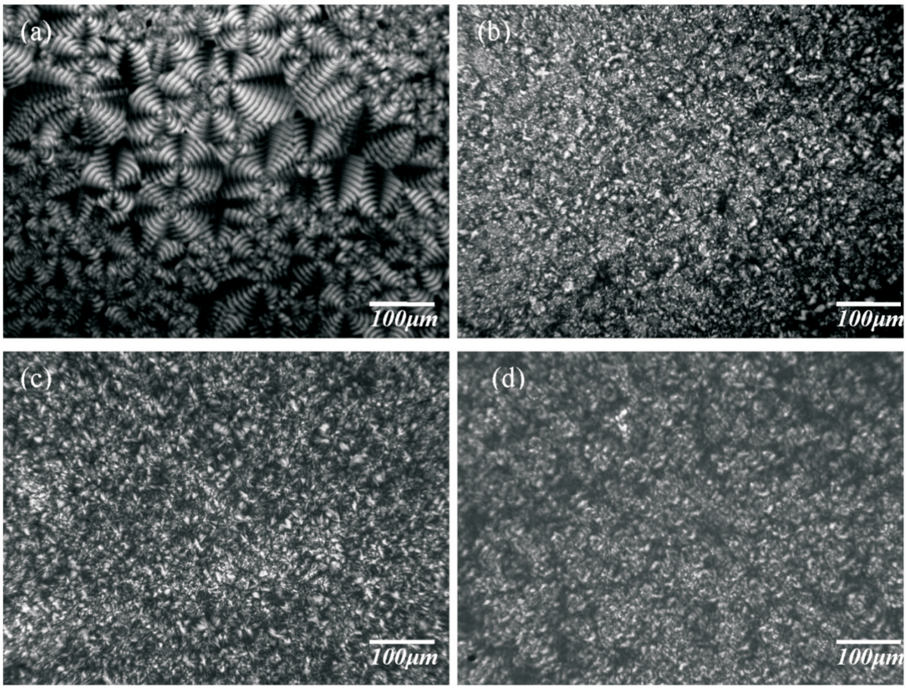

Figure 6. Optical micrographs of banded spherulitic structures of P(3HB) in PEO/P(3HB) blends crystallized at 50 °C, PEO/P(3HB) = (a) 0/100 (b) 20/80 (c) 50/50 (d) 80/20.

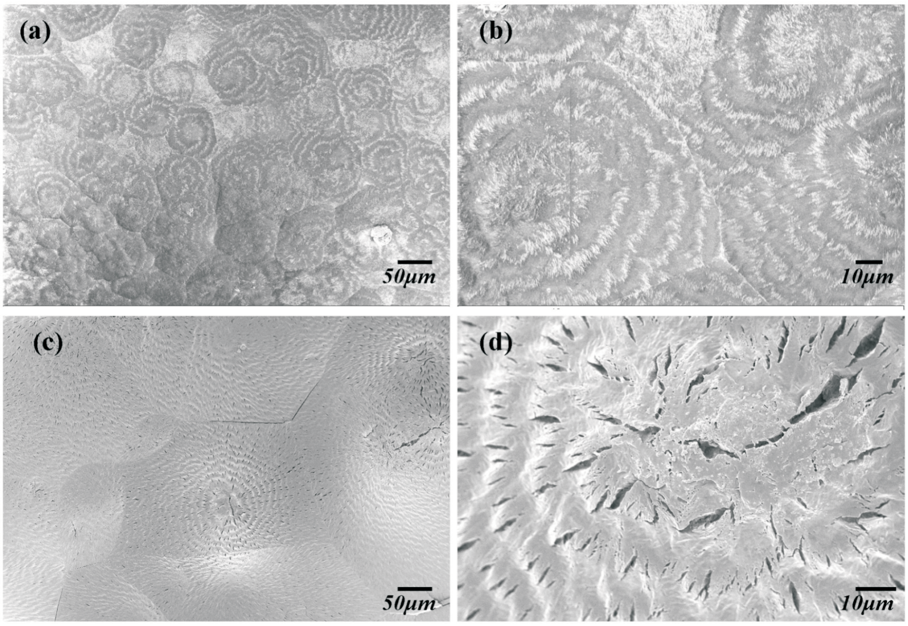

Figure 7. SEM micrographs of a PEO/P(3HB) blend (50/50) crystallized at 40 °C for three days. (a) × 500 (b) × 2000; the sample was then etched to remove PEO component by immersing in cold water at 5 °C for two days (c) × 500, (d) × 3000.

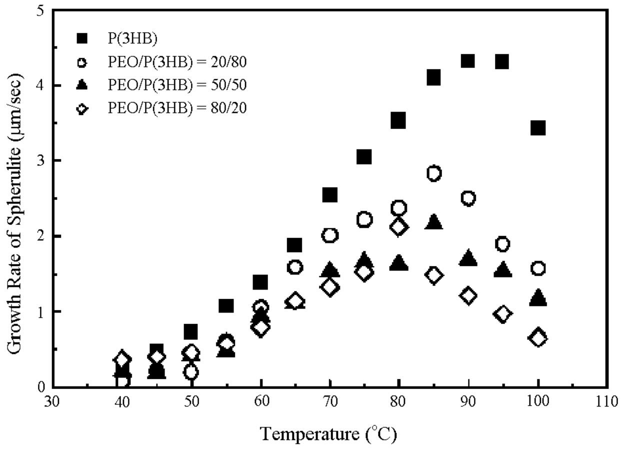

Figure 8. Spherulitic growth rate of P(3HB) with temperature for PEO/P(3HB) blends.

the crystallization window of a crystalline polymer lies between T_g and $T_m°$. When the crystallization temperature is located toward T_g, the crystallization kinetics is governed by the chain mobility, such that the rate increases with increasing crystallization temperature in this region. In contrast, when the crystallization temperature is located toward $T_m°$, the crystallization rate would be controlled by the thermodynamic driving force for crystallization. Because of interplay of these two factors, a maximum in crystallization rate at $T_{c,max}$ between T_g and $T_m°$ would be found. Compared to neat P(3HB), a gradual shift of this $T_{c,max}$ toward lower temperatures occurs in the blends with an increasing addition of PEO component. The shift in $T_{c,max}$ can be explained by the changes in T_g and $T_m°$ of the blends [30]. Furthermore, Figure 8 also shows the growth rate of P(3HB) crystallites decreases with increasing PEO content in the blends at all investigated crystallization temperatures above 50 °C (below 50 °C, it is very difficult to calculate the growth rate of P(3HB) crystallites because of the dense nucleation and competitive crystallization from PEO component). A dilution effect which diminishes the formation of a critical nucleus on the growth front of spherulites, and a decrease in the degree of undercooling due to the melting point depression can be applied to explain the decrease of growth rate in the miscible PEO/ P(3HB) blend. The enhanced chain mobility by the addition of PEO seems not to contribute large enough to change the decreasing trend of crystallization rate with PEO content. This result is not in agreement with the previous report [22], in which a maximum in growth rate is observed for the blend with a composition of PEO/P(3HB) = 50/50. This is probably a PEO oligomer having a molecular weight of 5,000 was used in that study, which the enhanced chain mobility has to be taken into account.

The experimental data of spherulitic growth rate were further analyzed according to the polymer-diluent theory [31,32]. The equation describes the growth rate of spherulites of a crystallizable polymer containing a second polymer acting as a diluent. The equation is shown below:

$$\begin{aligned}\beta &= \log G_{PHB} - \log\phi_2 + \frac{U^*}{2.3R(T_C - T_\infty)} - \frac{0.2T_m^o \ln\phi_2}{2.3\Delta T} \\ &= \log G_o - \frac{K_g}{2.3T_c\Delta Tf} \qquad (6)\end{aligned}$$

where G_o is a pre-exponential factor that is independent of temperature. The volume fraction of P(3HB), ϕ_2, is obtained using the densities of amorphous PEO and P(3HB) whose values are 1.08 g/cm^3 [33] and 1.17 g/cm^3, respectively [24]. The degree of undecooling, ΔT, is equal to ($T_m°$-T_c). The $U^*/2.3R(T_c$-$T_\infty)$ term contains the contribution arising from the diffusion of the crystallizable P(3HB) and diluent PEO involved in the crystallization. The quantity U* is the sum of activation energies of chain motion of P(3HB) and PEO in the melt and T_∞ is the temperature below which such motions cease ($T_\infty = T_g - C$, where C is a constant). The term f is a correction factor that accounts for the dependence of the heat of fusion on temperature and is written as $f = 2T_c/(T_m° + T_c)$. The parameter K_g is the nucleation factor expressed as:

$$K_g = \frac{nb_o\sigma\sigma_e T_m^o}{\Delta H_f k} \qquad (7)$$

where b_o is the thickness of a monomolecular layer, σ and σ_e are the lateral and folding surface energies, respectively, ΔH_f is the heat of fusion per unit volume, and k is the Boltzmann constant. According to the Hoffman theory [31], the value of n depends on the regime of crystallization. At high crystallization temperatures, each surface nucleation is followed by rapid completion of the growth strip prior to the next nucleation event. This is referred to regime I and n = 4. At lower crystallization temperatures, multiple surface nuclei occur and spread across the growth front together. The separation between nuclei decreases as the crystallization temperature decreases. This is regime II and n = 2. When crystallization occurs at still lower temperatures, the niche separation of multiple nuclei is of the order of the molecular width, when no more spreading takes place. This is regime III and n = 4.

The left-hand side of Equation (6) was plotted against $1/2.3T_c\Delta Tf$, with $T_m°$ values obtained from Table 1. Williams-Landel-Ferry values U* = 17.24 kJ/mol and $T_\infty = T_g - 51.6$ K were adopted for P(3HB) system. A good linear fit was obtained with the correlation coefficient value above 0.99. However, for the blends, U* was varied to maximize the correlation coefficient of the linear fit. The results are shown in Figure 9 and the values of K_g calculated from the slope are listed in Table 2. Barham et al. [24] found that P(3HB) crystallizes according to regime III at the crystallization temperatures used in this study (65~110 °C). Therefore, n = 4 according to Hoffman theory. However, the value of K_g decreases with increasing PEO content in the blends. To calculate the folded surface free energy σ_e, n = 4 was used for the pure

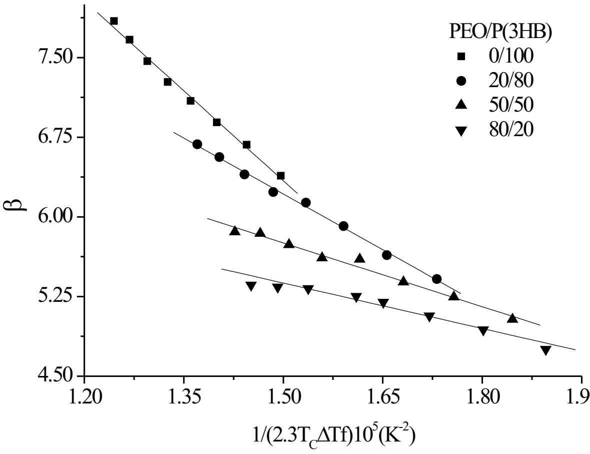

Figure 9. Plot of left-hand side of equation (6), $\beta = \log G_{PHB} - \log\phi_2 + \frac{U^*}{2.3R(T_C - T_\infty)} - \frac{0.2T_m^o \ln\phi_2}{2.3\Delta T}$, versus $1/2.3 T_c\Delta Tf$ to determine the nucleation factor K_g.

Table 2. Nucleation factor K_g and folded surface energy σ_e of P(3HB) crystals in PEO/P(3HB) blends

PEO/P(3HB)	U* (kJ/mole)	Log G_o (μm/s)	K_g (× 10^5 K^2)	σ_e (erg/cm^2)
0/100	17.24	14.81	5.648	47.2
20/80	16.11	11.47	3.504	30.2
50/50	15.06	8.756	2.001	17.4
80/20	12.34	7.518	1.427	12.5

P(3HB) and the blends, together with the values of b_o = 5.76 Å, σ = 29 erg/cm^2, $\Delta H_f = 1.85 \times 10^8$ J/m^3 [15]. The results are also listed in Table 2. The σ_e value for pure P(3HB) is fairly agreed to the value reported by Pearce et al. [15]. Yet, the value decreases with increasing PEO content. This behavior was also observed by Martuscelli et al. for the P(3HB)/poly(epichlorohydrin) blends [10].

4. Conclusions

Neat P(3HB) exhibits banded spherulitic texture as crystallized from the bulk, where a maximum growth rate of spherulites was found at 90 °C. At temperatures greater than 90 °C, band spacing increases and growth rate decreases with increasing crystallization temperature. When blended with a PEO having a molecular weight of 100,000, a single glass transition and a depression of melting point were observed for all the composition studied, proving that P(3HB) and PEO were miscible in the amorphous state. The interaction parameter χ_{12} calculated via the Nishi-Wang equation for this PEO/P(3HB) blend was -0.059. The results clearly show that though they were miscible, the interaction between P(3HB) and PEO was weak. In addition, as the same as increasing crystallization temperature over 90 °C, the addition of PEO decreases the spherulitic growth rate and increases the band spacing. This is attributed to the dilution effect that greatly diminishes the formation of a critical nucleus, and a decrease in the degree of undercooling due to the melting point depression. The experimental data of spherulitic growth rate were further analyzed according to the polymer-diluent theory. The nucleation factor K_g and the folded surface free energy σ_e of P(3HB) crystals are 5.648 $\times 10^5$ K^2 and 47.2 erg/cm^2, respectively. Both values decrease with increasing PEO content in the blends.

Acknowledgement

The authors wish to thank the financial support from National Science Council (NSC) in Taiwan. (Project No: NSC 93-2621-Z-032-002-)

References

[1] Lenz, R. W. and Marchessault, R. H., "Bacterial polyesters: Biosynthesis, Biodegradable Plastics and Biotechnology", *Biomacromol*, Vol. 6, pp. 1–8 (2005).

[2] Sudesh, K., Abe, H. and Doi. Y., "Synthesis, Structure and Properties of Polyhydroxyalkanoates: Biological Polyesters", *Prog Polym Sci*, Vol. 25, pp. 1503–1555 (2000).

[3] Lee, S. Y., Choi, J. and Wong H. H., "Recent Advances in Polyhydroxyalkanoate Production by Bacterial Fermentation: Mini-review", *Int J Biol Macromol*, Vol. 25, pp. 31–36 (1999).

[4] Braunegg, G., Lefebvre, G. and Genser, K. F., "Polyhydroxyalkanoates, Biopolyesters from Renewable Resources: Physiological and Engineering aspects", *J Biotechnol*, Vol. 65, pp. 127–161 (1998).

[5] Lee, S. Y., "Bacterial Polyhydroxyalkanoates", *Biotechnol Bioeng*, Vol. 49, pp. 1–14 (1996).

[6] Khambatta, F. B.; Warner, F.; Russell, T.; Stein, R. S., "Small-angle X-ray and Light Scattering Studies of the Morphology of Blends of Poly(-caprolactone) with Poly(vinyl chloride)", *Journal of Polymer Science, Polymer Physics Edition*, Vol. 14, pp. 1391–1424 (1976).

[7] Russell, T. P., Ito, H. and Wignall, G. D., "Neutron and X-ray Scattering Studies on Semicrystalline Polymer blends", *Macromolecules*, Vol. 21, pp. 1703–1709 (1988).

[8] Defieuw, G., Groeninckx, G. and Reynaers, H., "Miscibility and Morphology of Binary Polymer Blends of Polycaprolactone with Solution-chlorinated Polyethylenes", *Polymer*, Vol. 30, pp. 595–603 (1989).

[9] Keith, H. D. and Padden, F. J. Jr., "Spherulitic Crystallization from the Melt. I. Fractionation and Impurity Segregation and their Influence on Crystalline Morphology", *J. Appl. Phys*., Vol. 35, pp. 1270–1285 (1964).

[10] Paglia, E. D., Beltrame, P. L., Canetti, M., Seves, A., Marcandalli, B. and Martuscelli, E., "Crystallization and Thermal Behavior of Poly(D(-)3-hydroxybutyrate)/Poly(epichlorohydrin) Blends", *Polymer*, Vol. 34, pp. 996–1001 (1993).

[11] Sadocco, P., Canetti, M., Seves, A. and Martuscelli, E., "Small-angle X-ray Scattering Study of the Phase Structure of Poly (D-(-)-3-hydroxybutyrate) and Atactic

Poly(epichlorohydrin) Blends", *Polymer*, Vol. 34, pp. 3368–3375 (1993).

[12] Greco, P. and Martuscelli, E., "Crystallization and Thermal Behaviour of Poly(D(-)-3-hydroxybutyrate) based Blends", *Polymer*, Vol. 30, pp. 1475–1483 (1990).

[13] An, Y., Dong, L., Xing, P., Mo, Z., Zhuang, Y. and Feng, Z., "Crystallization Kinetics and Morphology of Poly(β-hydroxybutyrate) and Poly(vinyl acetate) Blends", *Eur Polym J*, Vol. 33, pp. 1449–1452 (1997).

[14] Chiu, H. J., Chen, H. L., Lin, T. L. and Lin, J. S., "Phase Structure of Poly(3-hydroxy butyrate)/Poly (vinyl acetate) Blends Probed by Small-angle X-ray Scattering", *Macromolecules*, Vol. 32, pp. 4969–4974 (1999).

[15] Pearce, R., Brown, G. R. and Marchessault, R. H., "Crystallization Kinetics in Blends of Isotactic and Atactic Poly(β-hydroxybutyrate)", *Polymer*, Vol. 35, pp. 3984–3989 (1994).

[16] Abe, H., Doi, Y., Satkowski, M. M. and Noda, I., "Miscibility and Morphology of Blends of Isotactic and Atactic Poly(3-hydroxybutyrate)", *Macromolecules*, Vol. 27, pp. 50–54 (1994).

[17] Iriondo, P., Iruin, J. J. and Fernandez-Berridi, M. J., "Thermal and Infra-red Spectroscopic Investigations of a Miscible Blend Composed of Poly(vinyl phenol) and Poly(hydroxybutyrate)", *Polymer*, Vol. 36, p. 3235 (1995).

[18] Xing, P., Dong, L., An, Y., Feng, Z., Avella, M. and Martuscelli, E., "Miscibility and Crystallization of Poly(β-hydroxybutyrate) and Poly(p-vinylphenol) Blends", *Macromolecules*, Vol. 30, pp. 2726–2733 (1997).

[19] Avella, M. and Martuscelli, E., "Poly-D-(-)(3-hydroxybutyrate)/Poly(ethylene oxide) Blends: Phase Diagram, Thermal and Crystallization Behaviour", *Polymer*, Vol. 29, pp. 1731–1737 (1988).

[20] Avella, M., Martuscelli, E. and Greco, P., "Crystallization Behaviour of Poly(ethylene oxide) from Poly (3-hydroxybutyrate)/Poly(ethylene oxide) Blends. Phase Structuring, Morphology and Thermal Behaviour", *Polymer*, Vol. 32, pp. 1647–1653 (1991).

[21] Avella, M., Martuscelli, E. and Raimo, M., "Fractionated Crystallization Phenomenon in Poly(3-hydroxybutyrate) Poly(ethylene oxide) Blends", *Polymer*, Vol. 34, pp. 3234–3240 (1993).

[22] You, J.-W., Chiu, H.-J. and Don, T.-M., "Spherulitic Morphology and Crystallization Kinetics of Melt-Miscible Blends of Poly(3-hydroxybutyrate) with Low Molecular Weight Poly(ethylene oxide)", *Polymer*, Vol. 44, pp. 4355–4362 (2003).

[23] Nishi, T. and Wang, T. T., "Melting Point Depression and Kinetic Effects of Cooling on Crystallization in Poly (vinylidene fluoride)-Poly(methyl methacrylate) Mixtures", *Macromolecules*, Vol. 8, pp. 909–915 (1975).

[24] Barham, P. J., Keller, A., Otun, E. L. and Holmes, P. A., "Crystallization and Morphology of a Bacterial Thermoplastic: Poly-3-hydroxybutyrate", *J. Mater. Sci.*, Vol. 19, pp. 2781–2794 (1984).

[25] Schultz, J. M., "Transient Effects in Crystallization of Polyethylene", *J Polymer Science- Polymer Physics*, Vol. 7, pp. 821–827 (1969).

[26] Xu, J., Guo, B.-H., Zhang, Z.-M., Zhou, J.-J., Jiang, Y., Yan, S., Li, L.,Wu, Q., Chen, G.-Q. and Schultz, J. M., "Direct AFM Observation of Crystal Twisting and Organization in Banded Spherulites of Chiral Poly(3-hydroxybutyrate-co-3-hydroxyhexanoate)", *Macromolecules*, Vol. 37, pp. 4118–4123 (2004).

[27] Hobbs, J. K., McMaster, T. J., Miles, M. J. and Barham, P. J., "Cracking in Spherulites of Poly(hydroxybutyrate)", *Polymer*, Vol. 37, pp. 3241–3246 (1996).

[28] Chiu, H. J. and You, J.-W., "Lamellar Morphology of Poly(3-hydroxybutyrate)/Poly(ethylene oxide) Blends as Studied via Small Angle X-ray Scattering", *J. Polym. Res.*, Vol. 10, pp. 79–85 (2003).

[29] Lotti, N., Pizzoli, M., Ceccoru, I. G. and Scandola, M., "Binary Blends of Microbial Poly(3-hydroxybutyrate) with Polymethacrylates", *Polymer*, Vol. 34, pp. 4935–4940 (1993).

[30] Pearce, R. P. and Marchessault, R. H., "Melting and Crystallization in Bacterial Poly(β-hydroxyvalerate),

PHV, and Blends with Poly(β-hydroxybutyrate-co-hydroxyvalerate)", *Macromolecules*, Vol. 27, pp. 3869–3874 (1994).

[31] Hoffman, J. D., "Regime III Crystallization in Melt-crystallized Polymers: the Variable Cluster Model of Chain Folding", *Polymer*, Vol. 24, pp. 3–26 (1983).

[32] Cimmino, S., Martuscelli, E., Silvestre, C., Canetti, M., de Lalla, C. and Seves, A., "Poly(ethylene oxide)/Poly(ethyl methacrylate) Blends: Crystallization, Melting Behavior, and Miscibility", *J. Polym. Sci., Polym. Phys.*, Vol. 27, pp. 1781–1794 (1989).

[33] Talibuddin, S., Wu, L., Runt, J. and Lin, J. S., "Microstructure of Melt-miscible, Semicrystalline Polymer Blends", *Macromolecules*, Vol. 29, pp. 7527–7535 (1996).

Manuscript Received: Dec. 4, 2005
Accepted: Dec. 20, 2005